Design and dynamic response analysis of rope laying system of roped type rice direct seeding machine

Zhang Baofeng, Song Yuqiu, Wu Liyan, Xin Mingjin, Ren Wentao*

(*College of Engineering, Shenyang Agricultural University, Shenyang 110161, China*)

Abstract: Rope laying mechanism is one of the important parts of roped type rice direct seeding machine. In order to solve the problems of breakage and loosening of seed rope during rope laying of the roped type rice direct seeding machine, a kind of rope laying mechanism composed of a rope disk, guiding wheels and a furrow opener was designed in this paper. The mechanism lays the rope by applying the friction between the rope and the soil. A simulation test of the rope laying system was carried out based on the Adams/Cable module for the first time to study the effect of wrap angle and the relative positions of the guide wheel on rope laying tension. The results showed that the smaller the wrap angle of the guiding wheel was, the less the rope tension would become. The validity of the simulation was proved by rope laying experiments and force analysis on the seed rope and the wheels. The minimal rope laying tension was obtained when the wrap angle of the bottom guiding wheel was 45°. Step response test showed that the rope laying system could satisfy the characteristics of first-order inertia process, and its amplification coefficient was 1.148, time constant was 0.174 s. Dynamic response analysis proved that the designed rope laying system could meet the design requirements and provide theoretical basis for design of roped type rice direct seeding machine and other related machinery.

Keywords: direct seeding of rice; rope laying system; simulation test; dynamic response

Citation: Zhang, B. F., Y. Q. Song, L. Y. Wu, M. J. Xin, and W. T. Ren. 2017. Design and dynamic response analysis of rope laying system of roped type rice direct seeding machine. International Agricultural Engineering Journal, 26(3): 120–129.

1 Introduction

Roped type direct seeding technology was first applied in western countries and it was mainly aimed at small seed crops such as vegetables (Lerink, et al., 2005; Henrik, 2006; Deppermann, et al., 2011; Deppermann et al., 2013). It was brought to Asia in 1961 and Nippon Company in Japan and Kon in Korea studied this technology (Kon, 1982; Park, 1986). The roped type rice direct seeding technology was first proposed by Ren (2005), and some related experimental researches were carried out and proved it is practical, seeds saving and more economical than normal direct seeding (Lv et al., 2008; Lv, 2008; Ren et al., 2009; Lv et al., 2010; Han, 2016; Zhang, et al., 2017; Lv, 2017). After developing several generations of sample machine, the roped type rice direct seeding machine mainly includes the following sections: ditching system, rope laying system, compacting system and soil covering system. As one of the key steps in roped type direct seeding, the rope laying system mainly guides seed rope disk to ditch stably based on the preset trajectory. In the process of rope laying, the rope should have good consistency and not easy to break and loosen, because the reliability of the rope laying system determines seeding quality. Zhang et al. (2006) designed a manual roped type rice direct seeding machine which rope laying device is driven by storage battery powered electric motor which is a kind of active rope laying system. The roped type rice direct seeding machine designed by Wang and Shang (2012) guided the seed rope to the field through a rope pipe. Song et al. (2014) designed a kind of automatic rope laying device, which can realize automatic rope laying by joint work of guiding pipe, rope pressing wheels and ditch pressing wheels. The mechanism can solve the problem of rope pressing by manpower and raise the rope laying efficiency, and has high demand on the

Received date: 2017-07-13 **Accepted date:** 2017-09-10
Corresponding author: Ren Wentao, Ph.D., professor, College of Engineering, Shenyang Agricultural University, 110866, China. Email: rwtsyau@sina.com

quality of tillage land. Zhu (2017) put forward a kind of seed rope and a plant method by putting the finished seed rope into the furrow and covered it with soil.

In conclusion, there are many researches on the related technologies and equipment of roped type rice direct seeding; however, there are few researches on dynamic response characteristics of rope laying system. Moreover, there are no researches on the effect of guiding angle and the relative position of guiding wheel on the rope laying tension. For the present roped type rice direct seeding machine, a direct connection was applied generally between the rope disk and rotating shaft, therefore, unstable friction occurs during seeding. In seed rope laying process, if the damping of the system is too high, the rope tension will be increased; besides, the inappropriate rope guiding mechanism may also lead to high tension on the rope. When rope tension increases to an ultimate value, the rope will break. Normally, rope breakage takes place at the start of working. Besides, if the damping of the system is too small, when the seeding machine stops, the rope disk may continue rotating for a period influenced by inertia, and the rope would be too long and become very loose so that it may affect seeding. To solve the existing problems of the rope system, a simulation test was made on the rope laying system of the seeder and rope tension under different guiding angles and penetration angles based on the Adams/Cable module and manually operated roped type rice direct seeding machine (Guo et al., 2016; Zhang et al., 2017). After verification tests on the module, the optimal parameters of the rope were determined. After step response test on the rope laying system, the rope laying system were determined to test if they could meet the design requirement (Kang, 2016). The study can offer reference to function improvement for roped type rice direct seeding machine.

2 Design of rope laying system and static force analysis of seed rope

The rope laying system can be divided into two types in terms of power sources: active rope laying system and passive rope laying system. However, there are cases when the seed rope is too long or too short and affect seeding, therefore, the rope laying method was changed to passive rope laying in newly designed machine (Ren, et al.,2014; Lv, 2017). Aiming at solving the problems in rope laying at present, the rope laying system proposed in this paper has the following design requirements: 1) the system should be simple enough and the maximum tension in the rope laying process should be as small as possible and less than the limit tension of the rope; 2) After the seeding machine stops, the rope length should be not more than 15 cm. The seed rope needs to have good continuity, should not broke and slacken. In this paper, a two-stage rope guiding mechanism was adopted in the system, it was mainly composed of a rope disk, guiding wheels a and b, as is shown in Figure 1. The rope reached ditch through guiding wheels a and b. After covering with soil, there was friction between the rope and soil. When the seeder walked ahead, influenced by the friction, the rope disk rotated and laid the rope.

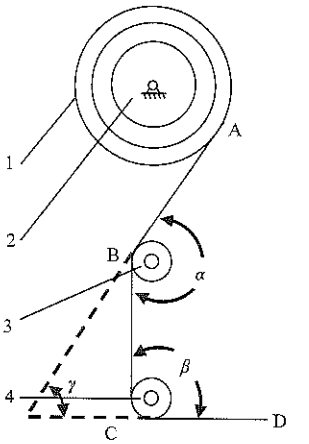

1. Seed rope 2. Rope disk 3. Guiding wheel a 4. Guiding wheel b

Figure 1 Structure of the rope laying system

The force analysis on seed rope and guiding wheel a was shown in Figure 2. A small section of seed rope *ds* on the wheel was randomly selected, and force analysis was done by microelement method. The width of the center angle of *ds* is $d\theta$, and the tensions at the two ends were T and $T + dT$, the elasticity between the rope and the wheel is dN, the sliding friction is df, and the weight of the rope is small and can be ignored, and the gravity on *ds* is not taken into consideration. Based on balance of forces, and:

$$(T+dT)\cos\frac{d\theta}{2}=T\cos\frac{d\theta}{2}+df \tag{1}$$

Since θ is very small, thus $\cos\frac{d\theta}{2}\approx 1$, and substitute it into Equation (1) and:

$$dT = df$$

Integrate two sides of the equation and get:

$$\int_0^{\theta} dT = \int_0^{\theta} df \tag{2}$$

That is:

$$T_{BC} - T_{AB} = \int_0^{\theta} df = f_1 \tag{3}$$

$$f_1 = \mu \cdot N \tag{4}$$

$$N = (T_1 + T_2) \cdot \sin\frac{\theta}{2} \tag{5}$$

Equations (3), (4) and (5) show that, the smaller θ is, the smaller the friction between seed rope and guiding wheel would be. When the angle of the guide rope is constant, the larger the diameter of the guide wheel is, the bigger the arc length of guiding wheel of the rope round. Therefore, the sliding friction will increase. Besides, the rotational inertia of bigger guiding wheel is bigger, and needs to be driven by larger friction. Therefore, the diameter of the guide rope wheel designed in this paper is 15 mm. The vertical distance of guiding wheels a and b is the height of furrow opener curve, which is 100 mm. The guiding wheels a and b were placed on the same vertical line in the initial design, and the position parameters were optimized by experiment.

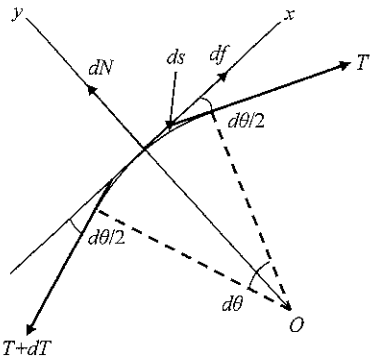

Figure 2 Force analysis of seed rope

3 Materials and method

3.1 Simulation test of rope laying based on Adams/Cable

3.1.1 Establishment of the test model

The simulation of the rope laying systems was carried out with Adams/Cable and the seed rope was simplified as a uniform cable. Since the rope weight per unit length was very small, and there was no need to study the swaying status of the rope, the "simplified" method in rope generation method was adopted in the simulation. In order to simplify the calculation model, only a two-dimensional force analysis was made on the rope laying system, and the axial translation of rope disk was not taken into consideration. In building the rope laying model, two fixed pulleys were used to represent guiding wheels a and b; two dummy balls represented the starting and end points of the rope laying mechanism, which were set at the center points of the two dummy balls.

The full-load diameter of the rope disk was 240 mm, no-load diameter of 80 mm, and the changing length of the radius of 80 mm. Since the diameter of the rope disk would decrease in laying rope, in order to simulate this change, a certain horizontal velocity v_0 was exerted on the dummy ball, and the rope laying speed was controlled by applying the winch order. A horizontal constant force F was exerted on the dummy ball at the end point to simulate the friction between the soil and seed rope. The simplified model of rope laying system is shown in Figure 3.

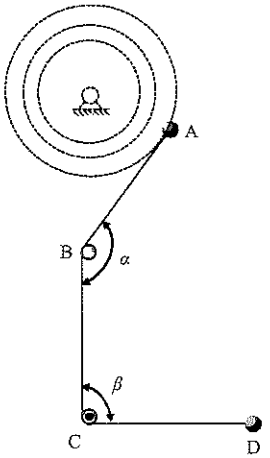

Note: A. Starting point of rope laying; B. Guiding wheel a; C. Guiding wheel b; D. Pulling end.

Figure 3 Model of rope laying system

3.1.2 Test method

In seeding, there are two types of motion between guiding wheels and seed rope: sliding and rolling, therefore, "Fixed" pully type was adopted to simulate the sliding movement between the seed rope and guiding wheels, and "revolute" pully type was adopted to simulate the rolling movement between seed rope and guiding wheels. Simulation parameters are shown in Table 1. Taking rope laying speed, type of guiding wheels as test variables, pulling force on rope as the test index, six groups of tests were carried out and each group of tests were repeated for five times.

Table 1 Parameter settings of seed rope laying simulation

Constraints and driving settings		Parameter settings of seed rope and guiding wheels	
Related components	Constraint type (parameters)	Friction coefficient	0.3
Rope laying end and ground	Horizontal sliding pairs	Critical contact velocity, mm/s	5
Pulling end and ground	Horizontal sliding pairs	Contact rigidity	1E4
Gravity	Closed	Type of guiding wheels	Fixed, Revolute
Rope laying speed, mm/s	300, 500, 700	Carrier of guiding wheels	Ground
Pulling force, N	10	Rope type	Simplified
Speed of rope laying end, mm/s	10	Simulation time, s	15

Note: In order to get the changing trend of the forces on the rope, the rope laying speed in the simulation test is higher than the speed of radius reduction of rope disk in practical work.

3.2 Test of tension in rope laying

3.2.1 Test materials

Test instruments and equipment are as following: (1) Rope tension collection system: a) QLYS-type tension sensor and QL-BSQ-8-type transmitter with measuring range of 0-50 kg, precision of 0.1%, the input voltage is direct current 24 V, which are produced by Qi Li sensor systems engineering co. LTD in Bengbu; b) 24 V power pack; c) JKU12 Data Acquisition Card which produced by Labjack company in USA; d) software program of a dual channel storage oscilloscope; (2) Testing device of pulling speed: ultrasonic distance measuring sensor US-100 which was produced by Yongye electronic technology co. LTD in Shenzhen; b) Arduino development board; c) SD card Module; (3) Testbed for rope laying system; (4) Rope disk; (5) Computer. The distance measuring range of the ultrasonic sensor is 0.024.5 m, input voltage is 2.4-5.5 V, quiescent current is 2 mA, working temperature is –20°C-70°C with temperature compensation function.

The design of rope laying system testbed: the testbed is composed of a body frame and moveable guiding wheels. The size of the testbed is 400×400×1500 mm. The rope disk is fixed at the top of the testbed through wheels and axles, and the guiding wheels a and b can move horizontally.

3.2.2 Test method

In order to test the impact of rope laying speed and angle on rope tension, rope guiding angle α and rope laying speed v were adopted as test variables, rope tension T was adopted as test index for a single-factor test, the test system and test scheme are shown in Figure 4. Refer to Figure 1, the position of guiding wheels a and b was adjusted to keep α was 180°, 165°, 150°, 140°, 135° respectively and β should be kept at 90°. When α = 180°, only the guiding wheel b was used for rope guiding. One end of the rope was connected in series with the tension sensor, the other end was connected with the ultrasonic sensor. After setting the initial position, a vertical baffle was placed at 2.4 m from the initial position for ultrasonic positioning. The rope laying speed was measured indirectly by the ultrasonic sensor; the sampling frequency of rope tension test system was 200 Hz. Since the rope was pulled by hands, the traction speed cannot be controlled with precision, therefore for each test, a period with stable speed was selected for rope tension analysis, and each test was repeated three times.

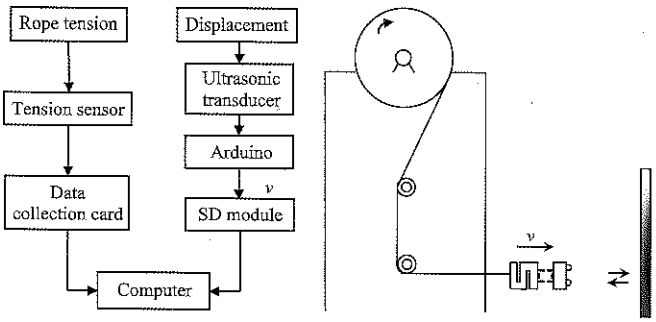

a. Seed rope tension test system diagram b. Connection diagram of the system

Figure 4 Seed rope tension test system diagram and connection diagram

Data processing: data processing was done by Excel 2007, then SPSS19 was used for statistical analysis, and Duncan method was used for significance testing, with significance level α=0.05.

3.3 Optimization test of rope laying system

3.3.1 Test model

Test model is the same with that in the rope laying simulation test.

3.3.2 Test plan

Figure 1 shows that:

$$\alpha+\beta=\pi+\gamma \tag{6}$$

The radius of the rope disk changed slowly in seeding, thus γ was regarded as a constant value in a short period of

time, namely section AB on the seed rope kept its position and the sum of α and β was a constant value. The test scheme and parameter settings are shown in Table 2 and Table 3, where, α varies within the range of 60°-180° along with the movement of guiding wheel b.

Table 2 Test scheme

Test variables		Test indexes
γ	45°, 60°, 75°, 90°	T_{AB}
α	60°-180°	

Table 3 Parameter setting of rope laying simulation test

Constraints and driving settings		Parameter settings of seed rope and guiding wheels	
Related components	Constraint type (parameters)	Friction coefficient	0.3
Rope laying end and ground	Fixed	Critical contact speed, mm/s	5
Rope laying speed, mm/s	100	Contact rigidity	1E4
Guiding wheel b and the ground	Horizontal sliding pairs	Type of guiding wheels	Fixed
Moving speed of guiding wheel b, mm/s	15	Carrier of guiding wheels	Ground
Pulling end and ground	Horizontal sliding pairs	Rope type	Simplified
Pulling force, N	10	Simulation time, s	15

3.4 Dynamic response analysis test of the rope laying system

3.4.1 Test materials

Instruments and equipment: (1) rope tension collecting system: (the same with the above). (2) Testing system of rotating speed; a) Hall sensor; b) Arduino development board; c) SD Module; d) Button magnet, diameter d = 6 mm; (3) Test bed for rope laying system; (4) Rope disk; (5) 1 kg weight; (6) Computer.

3.4.2 Test method

In this paper, step response characteristics were applied to study the rope laying system. The step response curve of the inertial element is an ascending curve of exponential function (Yang et al., 2016; Kang et al., 2016), which can be expressed by:

$$y(t) = Kx_0(1-e^{-t/T_c}) \quad (7)$$

Pretreatment of input signal: the input signal is a step function: $x(t)=x_0\times 1(t)$. Therefore, a weight of 1 kg was used in the test to give a constant excitation $F_0(t)$ to the system under the influence of gravitational force as system input.

Output signal collection: the output signal of the rope laying system is rope laying speed, namely, the rotating speed of rope disk, $\omega(t)$. The test used Hall sensor to measure the rotating speed of rope disk. The sensor moved in a circular motion (R=100) at one end face of the rope disk, with the same center with the rope disk. The circumference was divided into 24 equal parts, and a button magnet with a diameter of 6 mm was put on each knot, as is shown in Figure 5b. Then a Hall sensor was installed on the corresponding position on the testbed to receive electromagnetic signals and transmit the signals into the Arduino motherboard. Based on the equation $\omega(t)=\frac{\pi}{12t}$, the instantaneous angular velocity could be obtained, and signals of rotating speed were recorded into PC. The block diagram of signals of rotating speed and the connection diagram are shown in Figures 5a and 5c.

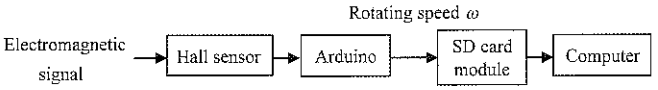

a. Block diagram of rotating speed signals

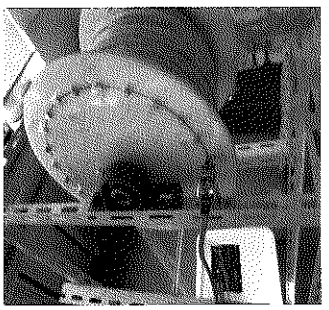

b. Rotating speed collection system for rope disk

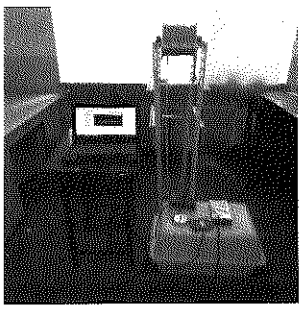

c. Rope laying test system

Figure 5 Dynamic response measurement system of seed rope

4 Results and discussion

4.1 Results and discussion of the rope laying simulation test

In the simulation test, in order to find out the position parameters of the guiding wheels at minimum rope tension, the pulling force at the rope end point was 10 N, and when the force on the starting point approximated to 10 N, the energy loss became less under such condition. Suppose that the minimum force that drives rotating of the rope disk was a constant, then the seeder could lead to minimum rope tension under such condition. The simulation results are shown in Figure 6. When there was sliding movement between the rope and guiding wheels, the tension on each section on the rope changed, and the section CD had the maximum tension, which was equal to the pulling force of

10 N; the tension of section BC was 6.4 N; the tension on the section AB was the minimum, but the tension on section AB increased linearly, and when the simulation came to an end, the tension on section AB was near to that of section BC, as is shown in Figure 6a. When there was only rolling between the seed rope and guiding wheels, each section on the rope was the same and equal to the pulling force, as is shown in Figure 6b, namely the pulling forces from both sides of the pulley were equal to each other. The reason was that, the starting point A of the rope had a horizontal-left speed, when α increased gradually, the wrap angle of guiding wheel a decreased gradually, and the friction between the rope and the guiding wheels also reduced, resulting in gradual increase of rope tension on section AB, but the wrap angle of guiding wheel b didn't change with time, so the tension on sections BC and CD kept constant. By ignoring the weight of seed rope, rope disk and guiding wheels, the rope laying speed didn't influence rope tension, since the sliding friction between the seed rope and guiding wheels was irrelevant to speed.

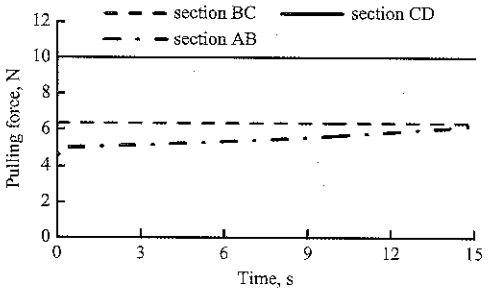

a. Tension on each section in sliding movement between seed rope and guiding wheels

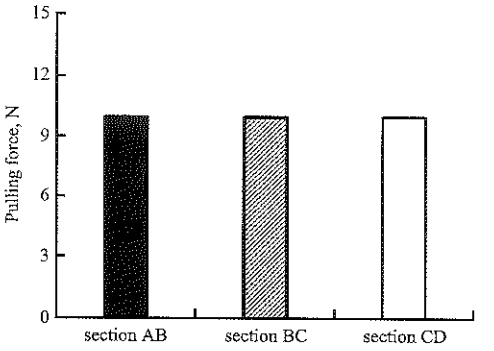

b. Tension on each section in rolling movement between seed rope and guiding wheels

Figure 6 Simulation results on rope tension

4.2 Results and discussion of the rope tension test

In order to test the validity of the rope tension test, a rope tension test was done on the solid model of the rope laying system. The measured tension was the tension on the section CD in Figure 1. The decrease of the tension on section CD in the rope tension test and the increase of tension on section AB in the simulation test are the same kind of conclusion. The results of rope tension test are shown in Figure 7. When α=180°, the tension value was the lowest. With the decrease of α, rope tension increased, showing that with the increase of wrap angle α of the guiding wheel a, the rope tension also increased in rope laying. The variance analysis showed that, $T_{\alpha 1}$was significantly lower than $T_{\alpha 5}$ (P<0.05), which was in line with the simulation test. Figure 7b shows the influence of rope laying speed on rope tension, where, Tv_5 is the maximum. But the variance analysis shows that, the differences among Tv_1, Tv_2, Tv_3, Tv_4, Tv_5 were insignificant, showing that the influence of rope laying speed on rope tension was also insignificant. This is in line with the influence trend of the rope laying speed on rope tension. The simulation test of rope laying based on Adams/Cable was proved to be effective.

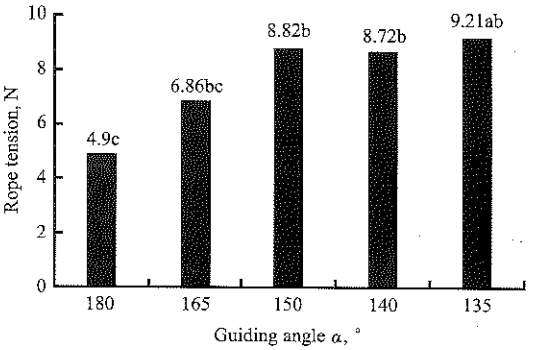

a. Rope tension at different guiding angles in rope laying

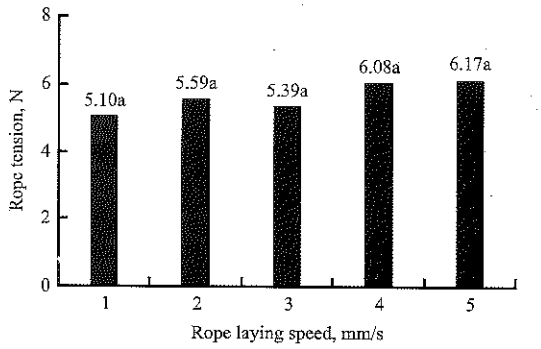

b. Rope tension at different rope laying speed

Figure 7 Results of seed rope tension test

4.3 Results and discussion of the rope laying structure optimization test

Based on the analysis above, the influence of the value of α and β on the friction between seed rope and guiding wheel is: the larger the angle between the seed ropes on

both sides of the guiding wheel, the smaller the friction is. Another simulation test of rope laying system was performed to optimize the position relationship of guiding wheels and the seed rope with a minimum friction between them. As is shown in Figure 8, with different γ angles, the tensions of section AB had the same shapes of curves, which went up with the increase of the wrap angle of guiding wheel a, and the tension of section AB reduced before an increase. This illustrates that when γ keeps constant, there was an optimum position to reach the maximum tension of section AB of the rope in simulation, in other words, the rope tension was the minimum in working. Besides, with the increase of the angle γ, the maximum value of AB section of the rope was also increasing gradually.

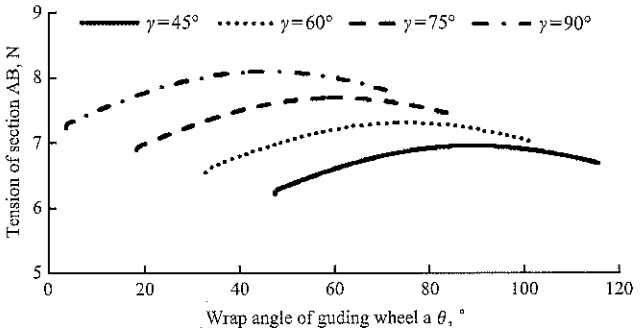

Figure 8 Comparison of simulation test results

θ_{a1} - θ_{a4}, θ_{b1} - θ_{b4} were used to represent γ=45°, γ=60°, γ=75°, γ=90°, which were the wrap angles of guiding wheel a when the section AB of the seed rope had the maximum tension, and:

$$\begin{cases} \theta_{a1} = 89.12° \\ \theta_{a2} = 74.80° \\ \theta_{a3} = 60.29° \\ \theta_{a4} = 45.25° \end{cases}$$

Substitute them into Equation (6) and get:

$$\begin{cases} \theta_{b1} = 45.88° \\ \theta_{b2} = 45.20° \\ \theta_{b3} = 44.71° \\ \theta_{b4} = 44.75° \end{cases}$$

For different γ angles, when section AB of the seed rope had the maximum tension, the wrap angles θ_a were different for the guiding wheel a, but the wrap angles of guiding wheel b were almost the same, at about 45°, showing that in the simulation test, for any values of γ angle, when the wrap angle θ_b of the guiding wheel b was about 45°, the AB section of the seed rope had the maximum tension. After rounding off the value, the following can be got:

$$\theta_b = 45°$$

Namely,

$$\beta = 180° - \theta_b = 135°$$

At this time the rope tension was the minimum, based on the optimized result of the curve of the furrow opener blade (Zhang et al., 2017), the overall structure of the rope-guided furrow opener is shown in Figure 9.

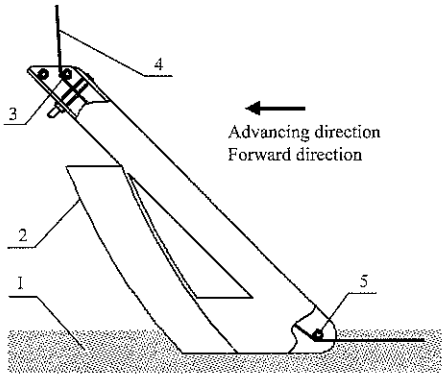

1. Soil 2. Blade of furrow opener 3. Guiding wheel a 4. Seed rope 5. Guiding wheel b

Figure 9 Structural diagram of rope-guided furrow opener

4.4 Results and discussion of the dynamic response test

4.4.1 Establishment of the transfer function model of the rope laying system

Set system input as rope tension of AB section in Figure 1, and system output as rotating speed of the rope disk, the rope disk diameter R reduced with seeding, thus the rotary inertia of the rope disk J would also change with time. According to moment of momentum theorem, the differential equation of the rope laying system was obtained:

$$F(t)R(t) = c\omega(t) + J(t)\dot{\omega}(t) \quad (8)$$

where, F(t) is the tension of AB section of the rope, N; $\omega(t)$ is the rotating speed of the rope disk, rad/s; R is radius of rope disk, m; J is rotary inertia of the system, kg·m^2; c is the equivalent coefficient of friction of the system, Nm/rad·s^{-1}.

Equations (8) show that, the differential equation is first order differential equation with variable coefficient, which is corresponding with linear time-variant system (Yang, 2016). Considering that the radius and weight of the rope disk would not change greatly, therefore the

model was simplified to first order differential equation with constant coefficients:

$$F(t)R = c\omega(t) + J\dot{\omega}(t) \tag{9}$$

Then the Laplacian transformation was applied on Equation (9) and the transfer function of the rope laying system that taking rope tension as input and rotating speed of rope disk as output was obtained:

$$G(s) = \frac{W(s)}{F(s)} = \frac{R}{c + Js} \tag{10}$$

Let $K = \frac{R}{c}$, $T_c = \frac{J}{c}$, and Equation (10) can be changed to:

$$G(s) = \frac{W(s)}{F(s)} = \frac{K}{1 + T_c s} \tag{11}$$

Equation (11) shows that, the rope laying system was in line with the first-order inertia link, K was amplification coefficient of the system and T_c was the time constant.

4.4.2 Determination of system parameters

The step response curve of the rope laying system is shown in Figure 10a, by applying the fitting tool Matlab/cftool (Xie, et al., 2012; Lin, et al., 2016), and taking Equation (7) as the theoretical regression equation, and the fitting result was obtained, as is shown in Figure 10b. Therefore, the step response equation of the rope laying system is:

$$y = 1.148x_0\left(1 - e^{-\frac{t}{0.174}}\right) \tag{12}$$

where, the confidence interval was 95%, regression coefficient R^2=0.92, showing a high fitting degree, namely K=1.148, T_c=0.174, thus the transfer function of the system is:

$$G(s) = \frac{W(s)}{F(s)} = \frac{1.148}{1 + 0.174s} \tag{13}$$

When the rope disk was fully loaded, it has greater rotary inertia, therefore, if the fully-loaded rope disk can meet design requirements, the rope laying system can also meet the design requirements, so checking calculation was done according to the size of the rope disk when it was fully loaded. According to rope tension, and:

$$T_{max}=\text{MAX}\{T_{AB}, T_{BC}, T_{CD}\}<[T] \tag{14}$$

where, T_{max} was the maximum tension of the seed rope, N; T_{AB}: tension of AB on the rope, N; T_{BC}: tension of BC on the rope, N; T_{CD}: tension of CD on the rope, N; $[T]$: maximum permissible stress of the rope, N.

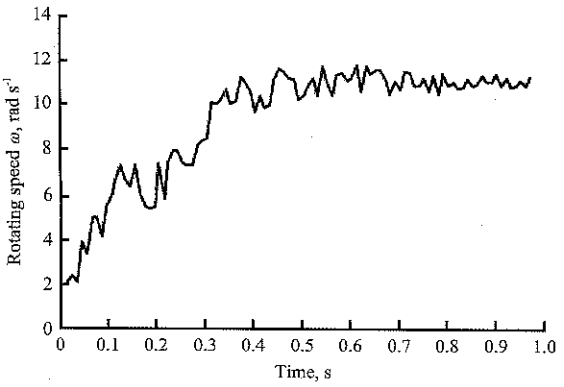

a. Step response curve

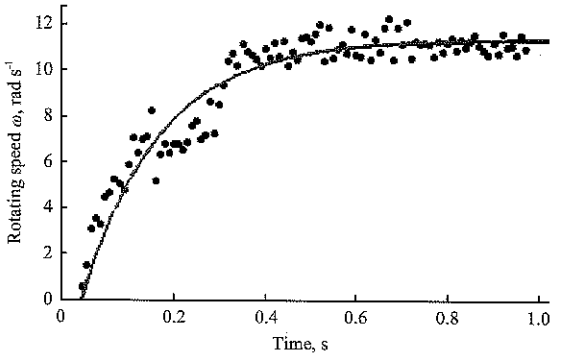

b. Fitting results

Figure 10 Result of the step response test

The seed rope pulling test shows that when it broke, the rope tension was influenced by the twist number in unit length, and the variation range was 27-43 N. It can be obtained by the simulation test that:

$$\text{MAX}\{T_{AB}, T_{BC}, T_{CD}\}=T_{CD}=T_{AB}+f_1+f_2 \tag{15}$$

where, f_1, f_2 are the frictions between the seed rope and guiding wheel a and b respectively, N. The average advancing velocity of the manpower roped type rice direct seeding machine was set as v_0=0.8 m/s, and the angular velocity $\omega=v_0/R$=6.67 rad/s. The Laplace transform of the transfer function showed that, the rope tension of section AB of the rope at this time was about 5.8 N. Besides, the frictional resistance on the rope made by the optimized guiding wheel was about 2 N, and T_{max}=5.8+2=7.8 N < $[T]$, showing that no rope breakage would occur and the system could meet the design demand.

After the seeder stopped going forward, it can be regarded that the seed falling length could meet the law of uniformly retarded motion.

$$x = \frac{1}{2}v_0 t \tag{16}$$

where, x is length of the falling rope, m; v_0 is the advancing speed of the seeder, m/s; t is the time for rope disk to stop working, s.

The rope laying system demands that the rope falling length x should not exceed 15 cm after the seeder stops moving forward, and substitute it into Equation (16) and get t=0.375 s, showing that within 0.375 s after the seeder stopped moving forward, the rope disk stopped working, and could meet the design requirements. And the time constant of the rope laying system T_c=0.174<t. In conclusion, the rope laying system can meet the design requirements.

5 Conclusions

1) In this paper, a kind of rope laying device composed of a rope disk, guiding wheels a and b was designed, and the device could realize synchronous rope laying by the friction between soil and the seed rope in soil.

2) Based on Adams/cable module, a simulation test was made on the rope laying system. The simulation results and theoretical analysis proved the significant influence of position of guiding wheels on rope tension, and the smaller the wrap angle of the guiding wheel is, the smaller the frictional resistance is, and the more rope tension was reduced in rope laying; rope laying speed had no influence on rope tension proving the effectiveness of the simulation analysis.

3) By applying the simulation analysis result and taking the rope guiding angle and wrap angle of the guiding wheel as test variables, the position relationship between rope disk and guiding wheels when the rope tension was the minimum during rope laying was obtained. When the angle γ between seed rope and the horizontal direction kept constant, the rope tension was the smallest when the wrap angle of the guiding wheel b was 45°, and on this basis, the position of guiding wheel b was adjusted to ensure the wrap angle was 45° in rope laying.

4) Through analytical method, the transfer function model of the rope laying system was determined as the first-order inertia mode. Through the step response test, the amplification coefficient of the transfer function of the system was determined as 1.148 and the time constant was 0.174. After considering design requirements and checking, the time for rope disk in stopping working Tc was less than the the required time t in design, the maximum tension of the rope T_{max} was less than the rope limit tension[T], indicating that the system could meet the design requirements.

The symbols in this paper are as follows:

α: the angle between sections AB and BC on the rope, degree;

β: angle between section BC and horizontal direction, degree;

γ: angle between section AB on the seed rope and vertical direction, degree;

F: external force in rope laying simulation, N;

v: rope laying speed, mm/s;

$T_{\alpha i}$: tension of section AB on the rope when dealing with the i-th α, N;

T_{vi}: tension of section AB on the rope when dealing with the i-th$v$, N;

T_{max}: the maximum tension of the seed rope, N;

T_{AB}: tension of section AB on the rope, N;

T_{BC}: tension of section BC on the rope, N;

T_{CD}: tension of section CD on the rope, N;

[T]: maximum permissible stress of the rope, N;

$\omega(t)$: rotating speed of the rope disk, rad/s;

K: amplification coefficient;

T_c: time constant of the system;

f_i: friction between the i-th rotary pipe and rope, N;

μ: coefficient of dynamic friction;

θ: wrap angle of the guiding wheel, degree;

$\theta_{\alpha i}$: wrap angle of the guiding wheel at the i-th γ treatment when the tension of AB section reaches maximum, degree;

θ_{bi}: wrap angle of the guiding pipe b at the i-th treatment when the tension of AB section reaches maximum, degree;

x: length of falling rope, m;

v_0: advancing velocity of the seeder; m/s;

t_s: time of stopping the rope disk, s;

R: radius of rope disk, m;

J: rotary inertia of the system, kg*m^2;

c: equivalent friction coefficient of the rope laying system, Nm/rad·s^{-1}.

[References]

[1] Deppermann, K. L., B. J. Forinash, T. Frey, and M. Mcnabnay. 2011. Seed tape planter. WO Patent 2011/119391 A1, filed 2011-03-16, and issued 2011-09-29.

[2] Deppermann, K. L., J. F. Brian, F. Travis, and M. Marcus. 2013. US Patent 2013/0152836 A1, filed and issued 2013-7-20.

[3] Guo, W., S. Li, and L. Ma. 2016. ADAMS 2013 Advanced application tutorial with Examples. *Beijing*: *China Machine Press*.

[4] Henrik, A. P. 2007. A germinating unit as well as a seed tape including several of such germinating units successively arranged. WO Patent 2007/065436A1, filed 2006-12-30, and issued 2007-06-14.

[5] Han, S. 2016. Improved design and Experimental Study on rice seed rope direct sowing machine. D.S. thesis, Shenyang Agricultural University.

[6] Kang, J., S. Li, X. Yang, L. Liu, and R. Zhu. 2016. Virtual simulation and power test of rotary ditcher based on multi-body dynamics. *International Agricultural Engineering Journal*, 4(25): 57–64.

[7] Kon, Y. 1986. Perforated seed tape. NZ Patent 201634A, filed and issued 1986-05-09.

[8] Lerink, P., and J. Wondergen. 2005. Device for planting seed(ling) tape. WO Patent 2005/72508 A1, filed 2005-01-26, and issued 2005-08-11.

[9] Lv, P. 2017. Design and study on walking rice rope direct seeding machine. M.S. thesis, Shenyang Agricultural University.

[10] Lv, X. 2008. Design and study on rice rope direct seeding machine. D.S. thesis, Shenyang Agricultural University.

[11] Lv, X., X. Cheng, and W. Ren. 2010. Design the key working part s of rice rope direct seeding machine. *Journal of Gansu Agricultural University*, 2010(3): 122–125, 130.

[12] Lv, X., X. Lv, and W. Ren. 2008. Analysis and research for the technology of rice direct sowing with seed rope. *Journal of Agricultural Mechanization Research*, 2008(01): 212–215.

[13] Park, D. C. 1986. Germinating tape of grass seed. KR Patent 890001102Y1, filed and issued 1986-09-17

[14] Ren, W., X. Li, H. Cui, and W. Liu. 2005. Effect of the technique of rice direct sowing with seeds twisted in paper rope on rice yield character. *Journal of Shenyang Agricultural University*, 36(3): 265–270.

[15] Ren, W., X. Lv, A. Kong, B. Zhang, H. Cui, and Y. Yang. 2009. Development of the taped type rice direct seeding machine. *Journal of Shenyang Agricultural University*, 40(1): 62–66.

[16] Ren, W., Y. Song, M. Xin, L. Wu, and H. Cui. 2014. Crop seed rope direct sowing machine.CN Patent CN103858566A, filed 2014-03-18, and issued 2014-6-18.

[17] Song, Y., W. Ren, M. Xin, and L. Wu. 2014. Automatic seed rope laying device. CN Patent CN 103858565 B, filed 2014-03-18, and issued 2014-06-18.

[18] Xie, Z., G. Li, H. Liu, P. Wu, and Z. Zheng. 2012. Matlab from zero to advanced. *Beijing*: *Beihang University Press*.

[19] Wang, J., and S. Shang. 2012. Development of plot precision planter based on seed tape planting method. *Transactions of the Chinese Society of Agricultural Engineering*, 28(65-71).

[20] Yang P., Weng S., and Z. Wang. 2016. Principles of Automatic Control. *Beijing*: *China Electric Power Press*.

[21] Zhang, Y. 2006. Study on development principle and testing for seed rope direct sowing machine of rice. M.S.thesis, Shenyang Agricultural University.

[22] Zhang, B., M. Xin, Y. Song, L. Wu, and W. Ren. 2017. Design of a manually operated rice seed rope planter. *International Agricultural Engineering Journal*, 26(1): 104–111.